

6-14-2017

Thermodynamically-Consistent Semi-Classical ℓ -Changing Rates

R. J. R. Williams
AWE plc, UK

Francisco Guzmán
University of Kentucky, francisco.guzman@uky.edu

N. R. Badnell
University of Strathclyde, UK

P. A. M. van Hoof
Royal Observatory of Belgium, Belgium

Marios Chatzikos
University of Kentucky, mchatzikos@uky.edu

See next page for additional authors

Right click to open a feedback form in a new tab to let us know how this document benefits you.

Follow this and additional works at: https://uknowledge.uky.edu/physastron_facpub

 Part of the [Physics Commons](#)

Repository Citation

Williams, R. J. R.; Guzmán, Francisco; Badnell, N. R.; van Hoof, P. A. M.; Chatzikos, Marios; and Ferland, Gary J., "Thermodynamically-Consistent Semi-Classical ℓ -Changing Rates" (2017). *Physics and Astronomy Faculty Publications*. 651.
https://uknowledge.uky.edu/physastron_facpub/651

This Article is brought to you for free and open access by the Physics and Astronomy at UKnowledge. It has been accepted for inclusion in Physics and Astronomy Faculty Publications by an authorized administrator of UKnowledge. For more information, please contact UKnowledge@lsv.uky.edu.

Authors

R. J. R. Williams, Francisco Guzmán, N. R. Badnell, P. A. M. van Hoof, Marios Chatzikos, and Gary J. Ferland

Thermodynamically-Consistent Semi-Classical ℓ -Changing Rates**Notes/Citation Information**

Published in *Journal of Physics B*, v. 50, no. 11, 115201, p. 1-9.

© 2017 IOP Publishing Ltd

After a 12-month embargo period from the publication of the Version of Record of this article, everyone is permitted to use, copy, and redistribute this article for non-commercial purposes only, provided that they adhere to all the terms of the Creative Commons Attribution-NonCommercial-NoDerivs 3.0 Unported license: <https://creativecommons.org/licences/by-nc-nd/3.0>

The document available for download is the authors' post-peer-review final draft of the article.

Digital Object Identifier (DOI)

<https://doi.org/10.1088/1361-6455/aa6f58>

PAPER

Thermodynamically-consistent semi-classical ℓ -changing rates

To cite this article: R J R Williams *et al* 2017 *J. Phys. B: At. Mol. Opt. Phys.* **50** 115201

Manuscript version: Accepted Manuscript

Accepted Manuscript is “the version of the article accepted for publication including all changes made as a result of the peer review process, and which may also include the addition to the article by IOP Publishing of a header, an article ID, a cover sheet and/or an ‘Accepted Manuscript’ watermark, but excluding any other editing, typesetting or other changes made by IOP Publishing and/or its licensors”

This Accepted Manuscript is © © 2017 IOP Publishing Ltd.

During the embargo period (the 12 month period from the publication of the Version of Record of this article), the Accepted Manuscript is fully protected by copyright and cannot be reused or reposted elsewhere. As the Version of Record of this article is going to be / has been published on a subscription basis, this Accepted Manuscript is available for reuse under a CC BY-NC-ND 3.0 licence after the 12 month embargo period.

After the embargo period, everyone is permitted to use copy and redistribute this article for non-commercial purposes only, provided that they adhere to all the terms of the licence <https://creativecommons.org/licenses/by-nc-nd/3.0>

Although reasonable endeavours have been taken to obtain all necessary permissions from third parties to include their copyrighted content within this article, their full citation and copyright line may not be present in this Accepted Manuscript version. Before using any content from this article, please refer to the Version of Record on IOPscience once published for full citation and copyright details, as permissions will likely be required. All third party content is fully copyright protected, unless specifically stated otherwise in the figure caption in the Version of Record.

View the [article online](#) for updates and enhancements.

Thermodynamically-consistent semi-classical ℓ -changing rates

R. J. R. Williams¹, F. Guzmán², N. R. Badnell³,
P. A. M. van Hoof⁴, M. Chatzikos², G. J. Ferland³

¹ AWE plc, Aldermaston, Reading RG7 4PR, UK

² Department of Physics and Astronomy, University of Kentucky, Lexington, KY 40506, USA

³ Department of Physics, University of Strathclyde, Glasgow G4 0NG, UK

⁴ Royal Observatory of Belgium, Ringlaan 3, 1180 Brussels, Belgium

Abstract. We compare the results of the semi-classical (SC) and quantum-mechanical (QM) formalisms for angular-momentum changing transitions in Rydberg atom collisions given in a series of papers by Vrinceanu et al, most recently Vrinceanu, Onofrio & Sadeghpour, *ApJ* **747**, **56** (2012), with those of the SC formalism using a modified Monte Carlo realization. We find that this revised SC formalism agrees well with the QM results. This provides further evidence that the rates derived from the QM treatment are appropriate to be used when modelling recombination through Rydberg cascades, an important process in understanding the state of material in the early universe. The rates for $\Delta\ell = \pm 1$ derived from the QM formalism diverge when integrated to sufficiently large impact parameter, b . Further to the empirical limits to the b integration suggested by Pengelly & Seaton, *MNRAS* **127**, 165 (1964), we suggest that the fundamental issue causing this divergence in the theory is that it does not fully cater for the finite time taken for such distant collisions to complete.

PACS numbers: 32.80.Ee, 34.10.+x, 34.50.Fa

Submitted to: *J. Phys. B: At. Mol. Opt. Phys.*

1. Introduction

There has been significant recent interest in the rates for **angular momentum** changing collisions of **low velocity ions with** Rydberg atoms. While this may seem a somewhat obscure corner of atomic physics, the time to pass through the ladder of high-angular momentum levels in highly excited atoms proves to be a bottleneck in the process of atomic (re-)combination in the early universe. The details of the ℓ -changing rates therefore have a major impact on our understanding of this important stage in cosmic development [1].

For this Stark mixing process to be the dominant, the impact parameter of the collision must be sufficiently large that both the orbital quantum number within the target does not change, and the field due to the collider ion must remain smaller than that of the host nucleus throughout the interaction [2].

The atomic physics of these rates can be calculated by a variety of approximations, **developing from classical orbit [3, 4, 5] to quantum orbit theory [6, 7, 8, 2, 9, 10]. In what follows we will refer to [2] and [10] as VF01 and VOS12, respectively.** In this paper, we will concentrate on the differences between the most detailed of these formulations, those based on **treating the response of the target orbital** using quantum-mechanical perturbation theory (QM) and classical trajectory theory (SC). As discussed elsewhere ([11, 12], and references therein), these theories result in predictions for integrated rates which differ by up to an order of magnitude, sufficient to have a major impact on the interpretation of observations. This difference is primarily the result of the different range in impact parameter over which $|\Delta\ell| = 1$ transitions are active in the different theories: the QM theory has a logarithmic divergence in transition rate, which requires a limit to be placed on the largest impact parameter for which collisions are active in causing transitions, while in the **SC approach as applied by VF01/VOS12**, this limit arises as a result of the finite domain in impact parameter over which a single collision can cause a complete $|\Delta\ell| = 1$ transition.

In this paper, we will present the results of calculations using the semi-classical theory of VF01, but using **Monte Carlo trajectory binning [13, 6]**. We find that with this alternative approach, the SC results agree well with those of the quantum theory. So far as there are differences, these are as would be expected when relating a quantum theory to its classical limit, and are consistent with the correspondence principle. When integrated over impact parameter, b , and a thermal spectrum of colliders, it is clear that the differences in rates computed using this modified SC approach and the original QM formalism will be minimal.

In Section 2 we present the background theory, and in Section 3 compare the QM transition probabilities with SC probabilities as calculated by VF01 and VOS12, and with our revised approach. In Section 4, we briefly discuss how the discretely-sampled VF01 SC approach can be made somewhat more accurate, and consistent with

the discrete detailed balance relations. Finally, in Section 5, we summarize our results, and discuss the processes which prevent the overall dipole transition rate from diverging in a plasma of finite density.

2. Theory

VF01 and VOS12 provide detailed formulae for the rates of transitions $\ell \rightarrow \ell'$ for precise values of ℓ, ℓ' . They derive their semi-classical formulae using approximations which correspond to the continuum limit $n, \ell, \ell' \rightarrow \infty$, with ℓ/n and ℓ'/n finite, and then apply them in the case of finite quantum numbers. They apply what they term as a microcanonical ensemble, sampling the fundamentally continuous classical-limit expressions at discrete values of incoming and outgoing angular momentum appropriate for the angular momentum quantum number. Using this procedure provides values for the overall collision rate which are finite for all $\Delta\ell$, as noted above.

The process of returning from the continuum to the discrete limit is not, however, unique. In the present paper, we use a method similar to that discussed by [13]. To ensure thermodynamic consistency for the derived total rates, it is better to follow a finite-volume formalism (see, e.g., [14]), where each of the discrete quantum numbers is taken to correspond to a finite range of continuum values. The simplest assumption which will ensure results are consistent with the thermodynamical equilibrium is to assume that the probability density of states in the continuum band corresponding to each of the aggregate states is internally in thermodynamic equilibrium. As there is no energy difference between states in the case considered by Vrinceanu et al., this corresponds to assuming a uniform population. This procedure provides results consistent with the thermodynamic requirements of unitarity and detailed balance and with the quantum and classical limits, as well as with usual practice in Monte Carlo simulation of off-lattice systems [15]. However, it leaves us looking to statistical physics, rather than numerical convention, to **understand how to prevent** the dipole transition rates **from diverging as a result of the long-range nature of the Coulomb interaction**.

For the standard quantum mechanical association of the radial quantum number n , the total angular momentum quantum number ℓ satisfies $0 \leq \ell \leq n - 1$. If we assume that each value of ℓ maps to a shell with total angular momentum between $\ell\hbar$ and $(\ell + 1)\hbar$, with a classical density of states $\propto \ell$ (which may be visualized as a two-dimensional polar coordinate system), then the area of this shell is $\propto 2\ell + 1$. This is consistent with the number of z -angular momentum eigenstates $|m| \leq \ell$ corresponding to each total angular momentum eigenstate. It results in a mean-squared angular momentum in the shell of

$$\langle L^2 \rangle = \left[\ell(\ell + 1) + \frac{1}{2} \right] \hbar^2, \quad (1)$$

which is a constant $\hbar^2/2$ greater than the value which enters in quantum mechanical calculations, $\langle L^2 \rangle = \ell(\ell + 1)\hbar^2$. For comparison, assuming that the total angular

Thermodynamically-consistent semi-classical ℓ -changing rates

4

momentum corresponding to a quantum number ℓ is exactly $\ell\hbar$ underestimates $\langle L^2 \rangle$ by $\ell\hbar^2$, which is a significantly larger error for large ℓ . [Taking the angular momentum for the discrete state to be $(\ell + \frac{1}{2})\hbar$ is more accurate, with the classical and quantum density of states being equivalent, and the mean-square angular momentum $\langle L^2 \rangle$ overestimated by $\hbar^2/4$.]

Transition probabilities in the finite volume regime can be derived from the semi-classical results of VF01/VOS12 by interpreting them as probability density functions in the continuum limit, so the transition probability from the state (n, ℓ) to (n, ℓ') becomes

$$\langle P^{\text{SC}} \rangle_{n\ell\ell'} = \frac{\int_{\ell/n}^{(\ell+1)/n} d\lambda \int_{\ell'/n}^{(\ell'+1)/n} d\lambda' P^{\text{SC}}(\lambda, \lambda', \chi) g(\lambda) g(\lambda')}{\int_{\ell/n}^{(\ell+1)/n} d\lambda g(\lambda)}, \quad (2)$$

where $g(\lambda) = 2\lambda$ is the classical density of states, normalized so that $\int_0^1 g(\lambda) d\lambda = 1$, and

$$P^{\text{SC}}(\lambda, \lambda', \chi) = \frac{2\lambda'/n}{\pi\hbar \sin \chi} \begin{cases} 0, & |\sin \chi| < |\sin(\eta_1 - \eta_2)| \\ \frac{K(B/A)}{\sqrt{A}}, & |\sin \chi| > |\sin(\eta_1 + \eta_2)| \\ \frac{K(A/B)}{\sqrt{B}}, & \text{otherwise,} \end{cases} \quad (3)$$

is the SC transition probability given by VOS12. In this expression, K is the complete elliptic integral,

$$A = \sin^2 \chi - \sin^2(\eta_1 - \eta_2), \quad (4)$$

$$B = \sin^2(\eta_1 + \eta_2) - \sin^2(\eta_1 - \eta_2), \quad (5)$$

$$\cos \eta_1 = \lambda, \quad (6)$$

$$\cos \eta_2 = \lambda', \quad (7)$$

and χ is given in terms of n and other implicit parameters of the collision by

$$\cos \chi = \frac{1 + \alpha^2 \cos(\sqrt{1 + \alpha^2} \Delta\Phi)}{1 + \alpha^2}, \quad (8)$$

$$\alpha = \frac{3Z_1}{2} \left(\frac{a_n v_n}{bv} \right), \quad (9)$$

where the swept angle $\Delta\Phi$ is assumed to be $-\pi$, **and the Stark mixing parameter α depends on the average radius and velocity, a_n and v_n of the target orbital, as well as the charge $Z_1 e$, impact parameter b and velocity v of the impinging ion.**

This procedure replaces the closed-form expressions of VF01 and VOS12 with a double integral, so is not as suitable for numerical work. However, it seems worthwhile

to compare the results with those of the discrete interpretation in order to inform possible modifications to the VF01/VOS12 formalism which might be made to ensure compatibility with the limit of thermodynamic equilibrium.

There are a number of desirable properties for any set of approximate transition probabilities. These include unitarity, i.e. that the system must reside in one of the angular momentum states at the end of the transition

$$\sum_{\nu} P_{n\ell\nu} = 1, \quad (10)$$

and detailed balance, i.e.

$$(2\ell + 1)P_{n\ell\ell'} = (2\ell' + 1)P_{n\ell'\ell}, \quad (11)$$

for the quantum level degeneracy $g(\ell) = 2\ell + 1$. Note that the sum for the unitarity requirement includes the probability that the scattering leads to no transition, $P_{n\ell\ell'}$ with $\ell' = \ell$. It is possible to determine this rate using the same analytic forms as for the ℓ -changing interactions, and this rate is included in the plots shown below.

The symmetry of the expressions for A and B in λ and λ' , together with the overall factor of λ' in equation (3), means that equation (3) satisfies the detailed balance relations *in the continuum limit*,

$$2\lambda P^{\text{SC}}(n, \lambda, \lambda') = 2\lambda' P^{\text{SC}}(n, \lambda', \lambda), \quad (12)$$

given the classical density of states $g(\lambda) = 2\lambda$. As a result of this, it is simple to verify that the phase-space average, equation (2), satisfies the discrete detailed balance relation

$$(2\ell + 1) \langle P^{\text{SC}} \rangle_{n\ell\ell'} = (2\ell' + 1) \langle P^{\text{SC}} \rangle_{n\ell'\ell}. \quad (13)$$

Beyond these absolute requirements, we also suggest that the rates should be subject to another statistical requirement for collisions at small impact parameter. For these scatterings, the output state of the interaction is dependent on complex interference phenomena, sensitive to many details of the atomic physics. However, the net effect of this complexity, when averaged over some small range of incoming particle properties, would be expected to be asymptotically close to the output states being in statistical equilibrium (cf., for the classical case, [16]). We therefore suggest that, in the limit of close scatterings $b \rightarrow 0$, the rates should be subject to an ergodicity property

$$\langle P \rangle_{n\ell\ell'} \simeq \frac{2\ell' + 1}{n^2}, \quad (14)$$

i.e. when the collider passes close enough to the core of the target atom, **in the Stark Adiabatic region**, the effect of the collision is to randomize the output state, when the input state is coarse-grained over a suitable domain. Of course, in reality scatterings will cease to be purely ℓ -changing in this limit. Even so, it is to be expected that the output state angular momentum will become statistically independent within the shell.

This requirement seems to be the best physical interpretation which can be put on the statement in [17], hereafter PS64, that in the core the scattering probability becomes a rapidly-oscillating function with mean value $\frac{1}{2}$. This is what would result from the core ergodicity principle in the case of a two-level system, so the core ergodicity principle seems like a reasonable generalization, agreeing with the work of PS64 at least in spirit. As we will see, it is also a reasonable description of what in fact happens when the quantum and shell-averaged classical transition probabilities are calculated in detail.

3. Results

3.1. Comparison of QM and SC theory for fixed quantum numbers

In Figures 1 and 2, we compare the quantum mechanical probability distributions with the SC transition probabilities sampled at specific ℓ , ℓ' . The QM dipole transition rates, $\Delta\ell = \pm 1$ decay slowly as b increases, which is the origin of the divergence of the rate integral for these transitions. The SC transition probabilities show sharp edges where the transitions first become allowed, for all $\Delta\ell$: the transition rates for all $\Delta\ell$ are similar, as there is nothing in the SC formulation which fundamentally distinguished a $|\Delta\ell| = 1$ transition from one with a larger change in angular momentum. There are also internal peaks for many cases, corresponding to orbital resonances. These are used by VOS12 to limit the domain over which $|\Delta\ell| = 1$ transitions are allowed, avoiding the divergence in the integrated transition rate found for the QM dipole transition rate.

It is clear that the SC transition probabilities cannot satisfy unitarity, as where any transition ceases to be allowed, there is no corresponding increase in the others. Indeed, at sufficiently large radii, the probability of no transition, $P_{n\ell\ell}$, increases above unity, which is inconsistent with usual definition of probability. The quantum transition probabilities do satisfy unitarity (note that the curves as plotted are divided by $2\ell' + 1$ to make the ergodicity property at small b more obvious, but this means that this summation property for the probabilities is less obvious as shown).

In Figures 3 and 4, we compare the quantum mechanical probability distributions with the SC probability distributions averaged over angular momentum shells. These plots are significantly more alike than those for the comparison between the quantum mechanical probability and the discretely-sampled SC transition probability. While there are no longer any sharp edges in the shell-averaged SC probabilities, for $|\Delta\ell| > 1$ they will be non-zero only within some range of α values. (The integration over a quantized shell width means that there is now a genuine distinction in qualitative behaviour between transitions with different $|\Delta\ell|$.) The shell-averaged SC probabilities also satisfy unitarity and the quantum-weighted detailed balance constraint.

Away from the region where the discretely-sampled transition probability is zero, the binning has a relatively minor effect, simply smoothing out the steepest peaks.

The general form of the transition probability distributions shown in these figures is of interest. Working from large b inwards, it is initially most likely that no change in ℓ

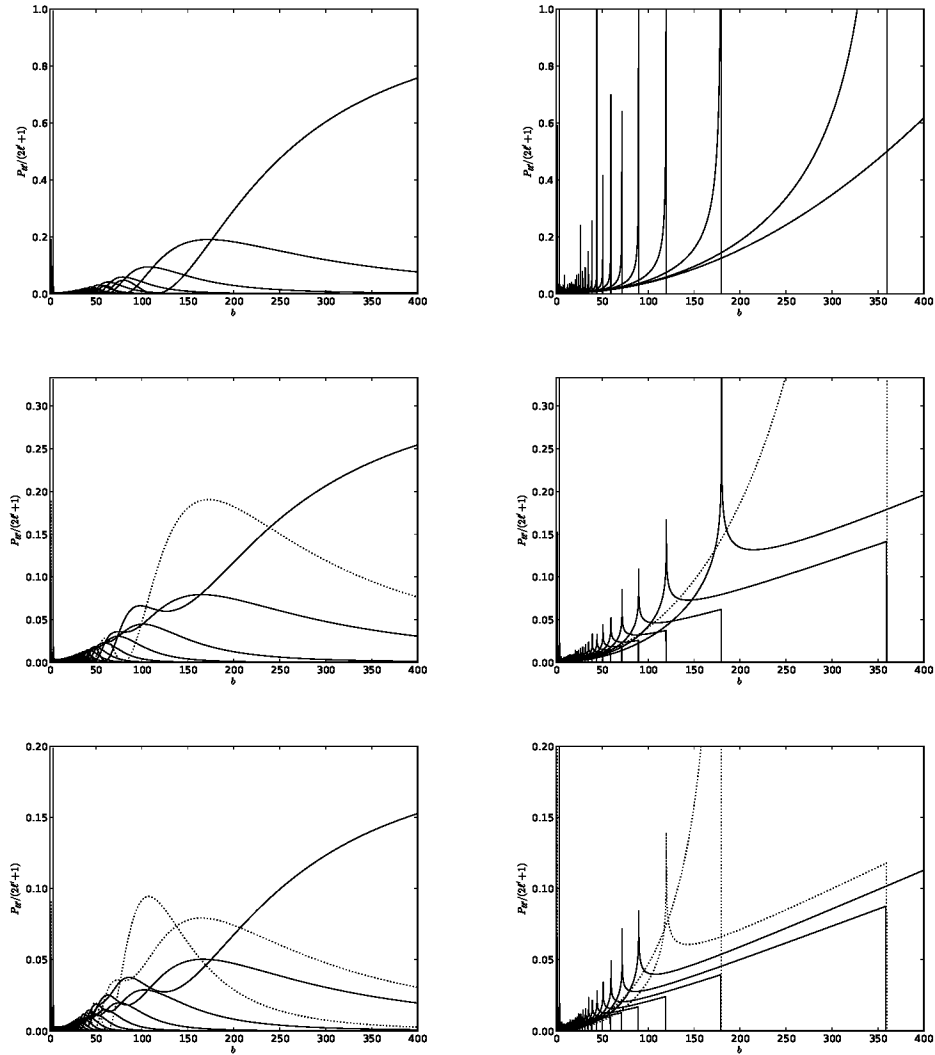


Figure 1. Plots of $P_{nl\ell'}/(2\ell'+1)$ vs b for $n=30$ and $\ell=0$ (first row), $\ell=1$ (second row) and $\ell=2$ (third row). The Stark parameter is $\alpha=6/b$. Left column is using the QM formalism, right is using the SC formalism. The highest curve at large b has $\Delta\ell=0$, larger $\Delta\ell$ curves appear in order as b reduces. Dotted curves are for $\ell'<\ell$.

will result. At least in the QM case, all other values of $\Delta\ell$ are possible, with probabilities reducing as $|\Delta\ell|$ increases. As b becomes smaller, the probabilities of the higher $|\Delta\ell|$ transitions increase, following a smooth power law dependency, until the statistical weight of the output state reaches a similar level to that of the $\Delta\ell=0$ transition. Thereafter, the probabilities are subject to significant oscillations, around an average level consistent with statistical balance, apart from a strong spike at the very smallest values of b . This suggests that the combination of the asymptotic behaviour at large b , the core ergodicity principle, and the fundamental requirements of unitarity and detailed balance, should be sufficient to provide thermodynamically-consistent estimates of the impact-parameter and thermal-averaged rates which would be acceptably accurate for many applications.

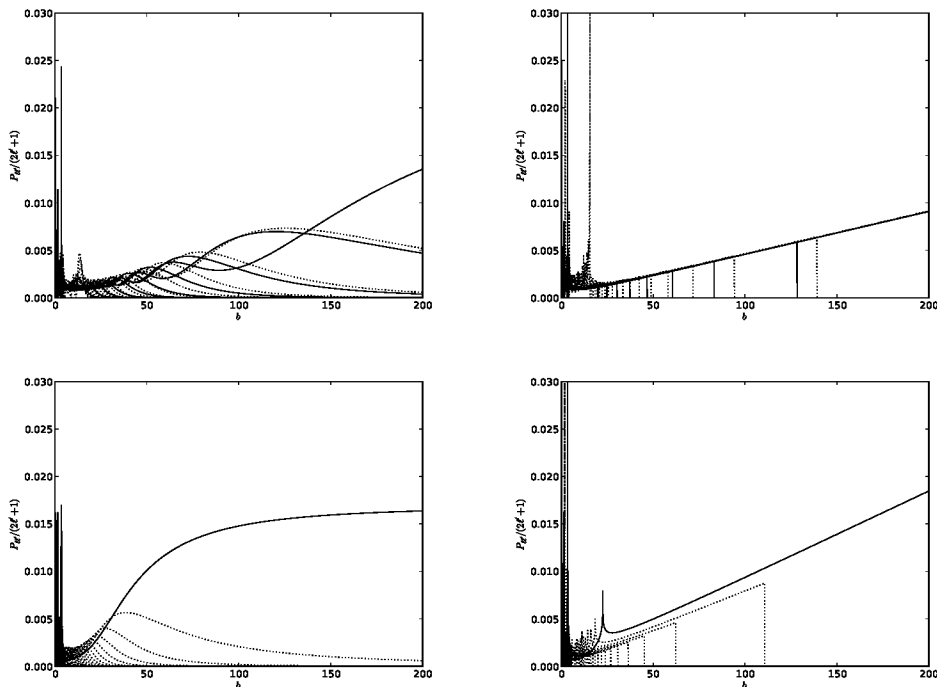


Figure 2. Plots of $P_{n\ell\ell'}/(2\ell'+1)$ vs b for $\ell = 20$ (first row) and $\ell = 29$ (second row). The n and α parameters are as in Figure 1. Left column is using the QM formalism, right is using the SC formalism. Dotted curves are for $\ell' < \ell$. **Note that there are no upward transitions for $\ell = 29$ due to the constraint that $\ell' < n$.**

3.2. The classical limit of the QM formalism

Having shown that the SC results can be made acceptably consistent with those of the QM formalism by an appropriate binning procedure, it is also of interest to demonstrate consistency in the opposite direction. To do this, in Figure 5, we compare the non-averaged SC probability for one transition with a series of QM results with quantum numbers increasing by factors of 2. As the quantum numbers increase, while maintaining their ratios, the QM results tend to the SC limit, with the resolution of sharp features, including the orbital resonances seen in the classical results, gradually improving. Oscillations remain within the classically-allowed range, and long tails in the classically-forbidden range. This combination of Gibbs phenomenon ringing and evanescent tunnelling behaviour, typical of the Airy function, is characteristic of the classical limit of quantum phenomena. The QM formalism remains accurate for all values of the quantum numbers, but the expressions for the rates become increasingly difficult to evaluate numerically.

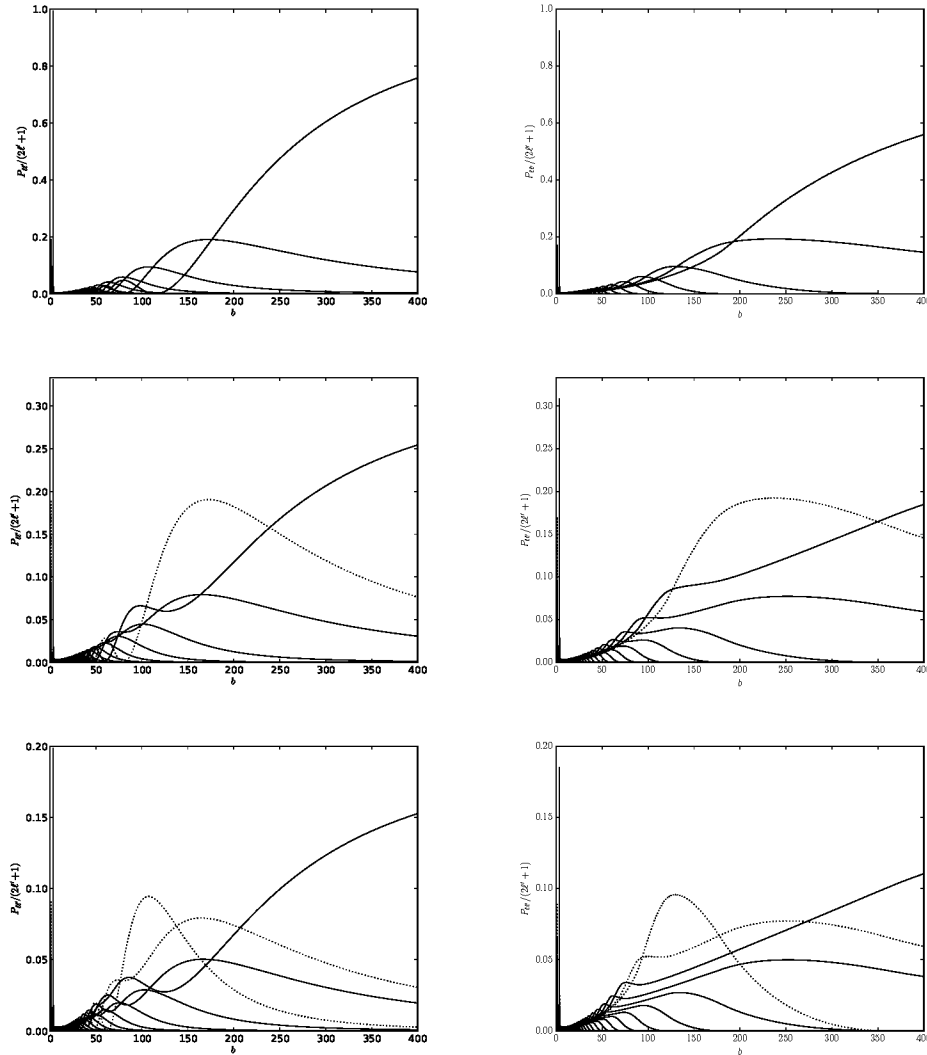


Figure 3. Plots of $P_{n\ell\ell'}/(2\ell'+1)$ vs b for $\ell = 0$ (first row), $\ell = 1$ (second row) and $\ell = 2$ (third row). Left column is using the QM formalism, right is using the SC formalism, averaged over shells. Dotted curves are for $\ell' < \ell$.

4. Use of semi-classical probabilities

The shell-sampled probabilities presented in the previous section are determined using a computationally expensive double integral. It may be possible to perform one or both of these integrals analytically, but numerical results were sufficient for the present analysis.

However, given that the use of a classical transition rate is already a significant approximation, using a point sample of the transition rate rather than an integral is likely to be an acceptable approximation, at least away from the case of $\Delta\ell = \pm 1$, $b \rightarrow \infty$. As these rates are being attributed to quantum mechanical rather than classical states, it makes sense to ensure the rates are chosen so as to satisfy quantum mechanical rather than classical statistics. The most consistent identification of quantum mechanical states

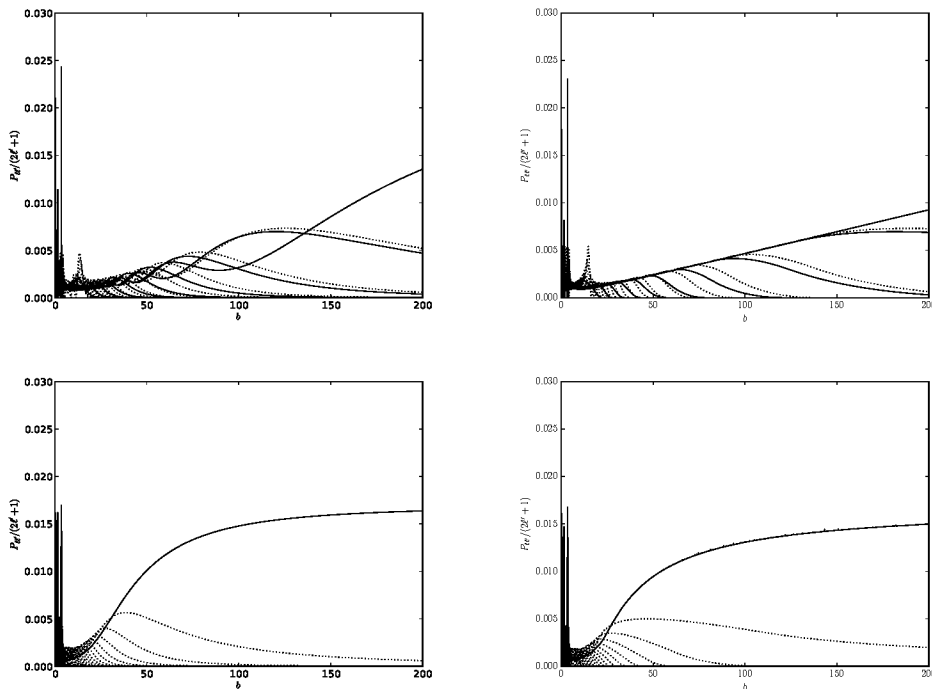


Figure 4. Plots of $P_{n\ell\ell'}/(2\ell'+1)$ vs b for $\ell = 20$ (first row) and $\ell = 29$ (second row). Left column is using the QM formalism, right is using the SC formalism, averaged over shells. Dotted curves are for $\ell' < \ell$.

with a continuum band has $\ell\hbar$ as the angular momentum at the innermost edge of the band. Hence, if a single value based on the classical transition probability is to be used for this quantum number, it will be accurate to a higher order if the angular momentum used in this expression is somewhat higher than $\ell\hbar$. In particular, in order to be consistent with the quantum mechanical detailed balance condition, the value $2\ell'+1$ should be used in the numerator of the prefactor of equation (6) of VOS12. This means that the $\ell \rightarrow \ell' = 0$ rates will not be strictly zero, as required by the expressions given by VF01. Given that VF01 provide expressions for the transition rate *out* of an $\ell = 0$ state, a zero inward rate is in clear violation of the detailed balance requirement.

The values used in the elliptic integral terms must be symmetric functions of ℓ, ℓ' , as is true for the expressions given. Ideally they should also be chosen to satisfy unitarity, but in reality the correction to the overall transition rates as a result of violating this constraint will be small compared to the other approximations underlying this approach. Using $\cos \eta_1 = (\ell + \frac{1}{2})/n$, etc., will be at least somewhat more accurate than without the $\frac{1}{2}$, and also means that the cases $\ell = 0, \ell' = 0$ do not require a special treatment.

5. Conclusions

We have shown that, by using an alternative form for the Monte Carlo realization, the results for the SC and QM formalisms described by VF01 and VOS12 can be

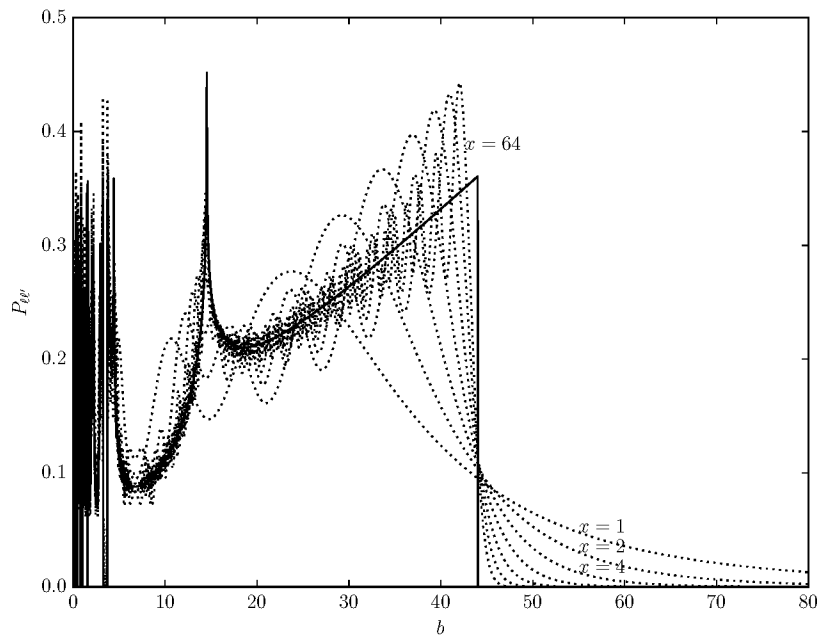


Figure 5. Comparison of the SC $P_{n\ell\ell'}$ vs b for $\ell = 2$, $\ell' = 4$, $n = 8$ transition probability (solid line), compared to a succession of scaled QM formalism probabilities $xP_{n\ell\ell'}$, with $\ell = 2x$, $\ell' = 4x$ and $n = 8x$, where $x = 1, 2, 4, 8, \dots, 64$. As the scaling factor x increases, the QM probabilities tend towards the SC results.

brought closely into line. As this is consistent with what is expected as a result of the correspondence principle, it provides further evidence that the results of the QM formalism of VF01 and VOS12 is accurate, and should be preferred over their SC formalism in regimes where their results differ significantly.

While finding agreement between the different forms of theory is satisfying, this does not take into account the major reason given by VF01 and VOS12 for preferring their semi-classical results, specifically the need for an outer limit to be imposed on the integration over impact parameters to prevent the total collision rate diverging for $\Delta\ell = \pm 1$ when using the QM theory. This type of divergence is common in other areas of collision rate physics (in particular, the two-body relaxation time, [18, 19]), so is not unexpected. PS64 give expressions for a variety of empirical limits to the range of b over which Stark mixing will be active, due to Debye screening, target atom state radiative lifetimes, and the lifting of degeneracy between the ℓ levels as a result of relativistic effects, or the finite core radius for target atoms of species heavier than H. The value of the outer cut-off is taken to be the most constraining of these processes. The logic here is similar to the outer limit applied to the Coulomb logarithm in other contexts, such as two-body relaxation in plasmas. The relevant Debye screening is that

which reduces the long-range field of the impinging ion (Debye screening of the charge of the target atom nucleus is in effect a continuum lowering process), and will be rapid for colliders with thermal velocities due to the high mobility of electrons.

Nevertheless, it is also worth noting that as b increases, so does the time over which the collision takes place: the treatment of collisions as independent events must therefore eventually become inaccurate. During the extended period taken to complete the most distant encounters, there will be time for many collisions at smaller impact parameters. While, at first order, the effects of collisions will superpose linearly, at sufficiently large b a limit will be reached where smaller impact parameter collisions together are sufficient to randomize the angular momentum of the target orbital **during the time over which the larger b interaction is taking place**. Once b increases above the level where this occurs, b_{eq} , the effect of collisions at larger impact parameter will be felt, in effect, as a superposition of $N_{\text{coll}} \sim \tau_{\text{coll}}/\tau_{\text{eq}}$ partial interactions adding in quadrature, rather than linearly (where τ_{coll} is the collision time at the large b of interest, and τ_{eq} is the collision time at the smallest radius leading to effective randomization). A reduction in contribution to the transition probability by $\sim N_{\text{coll}}^{-1/2} \propto b^{-1/2}$ at the largest b will be sufficient to prevent the weak logarithmic divergence in the overall rate. This is a somewhat academic argument, as **the plasma particle correlations underlying Debye screening will in general** result in more stringent limits to the range of b over which collisions are effective. Nevertheless, given that the agreement we now find between the SC and QM gives greater confidence in SC results for the Rydberg scattering problem, it may be possible to investigate the corrections required for these multiple interactions in a believable manner using explicit classical trajectory calculations.

Acknowledgements

We thank D. Vrinceanu and H. Sadeghpour for helpful responses to several queries about their published work, **and the referees for valuable suggestions**. Parts of this work have been supported by the NSF (1108928, 1109061, and 1412155), NASA (10-ATP10-0053, 10-ADAP10-0073, NNX12AH73G, and ATP13-0153), and STScI (HST-AR-13245, GO-12560, HST-GO-12309, GO-13310.002-A, and HST-AR-13914). MC has been supported by STScI (HST-AR-14286.001-A). PvH was funded by the Belgian Science Policy Office under contract no. BR/154/PI/MOLPLAN.

- [1] J. Chluba and R. A. Sunyaev. Induced two-photon decay of the 2s level and the rate of cosmological hydrogen recombination. *A&A*, 446:39–42, January 2006.
- [2] D. Vrinceanu and M. R. Flannery. Classical and quantal collisional Stark mixing at ultralow energies. *Phys. Rev. A*, 63(3):032701, March 2001.
- [3] I. C. Percival and D. Richards. Classical theory of transitions between degenerate states of excited hydrogen atoms in plasma. *Journal of Physics B Atomic Molecular Physics*, 12:2051–2065, June 1979.
- [4] A. K. Kazansky and V. N. Ostrovsky. Classical theory of ℓ -changing transitions in collisions between Rydberg atoms and ions. *Phys. Rev. A*, 52:R1811–R1814, September 1995.

- [5] A. K. Kazansky and V. N. Ostrovsky. Rydberg-atom - ion collision: classical theory of intrashell transitions. *Journal of Physics B Atomic Molecular Physics*, 29:3651–3672, August 1996.
- [6] AK Kazansky and VN Ostrovsky. Rydberg atom-ion collisions: Quantum theory of intrashell transitions. *Physical review letters*, 77(15):3094, 1996.
- [7] D. Vrinceanu and M. R. Flannery. Classical Stark Mixing at Ultralow Collision Energies. *Physical Review Letters*, 85:4880–4883, December 2000.
- [8] D. Vrinceanu and M. R. Flannery. LETTER TO THE EDITOR: Quantal Stark mixing at ultralow collision energies. *Journal of Physics B Atomic Molecular Physics*, 33:L721–L728, October 2000.
- [9] D. Vrinceanu and M. R. Flannery. LETTER TO THE EDITOR: Analytical quantal collisional Stark mixing probabilities. *Journal of Physics B Atomic Molecular Physics*, 34:L1–L8, January 2001.
- [10] D. Vrinceanu, R. Onofrio, and H. R. Sadeghpour. Angular Momentum Changing Transitions in Proton-Rydberg Hydrogen Atom Collisions. *ApJ*, 747:56, March 2012.
- [11] F. Guzmán, N. R. Badnell, R. J. R. Williams, P. A. M. van Hoof, M. Chatzikos, and G. J. Ferland. H, He-like recombination spectra - I. ℓ -changing collisions for hydrogen. *MNRAS*, 459:3498–3504, July 2016.
- [12] F. Guzmán, N. R. Badnell, R. J. R. Williams, P. A. M. van Hoof, M. Chatzikos, and G. J. Ferland. H-, He-like recombination spectra - II. ℓ -changing collisions for He Rydberg states. *MNRAS*, 464:312–320, January 2017.
- [13] R. L. Becker and A. D. MacKellar. Theoretical initial ℓ dependence of ion-Rydberg-atom collision cross sections. *Journal of Physics B Atomic Molecular Physics*, 17:3923–3942, October 1984.
- [14] Randall J LeVeque. *Finite volume methods for hyperbolic problems*, volume 31. Cambridge University Press, 2002.
- [15] David P Landau and Kurt Binder. *A guide to Monte Carlo simulations in statistical physics*. Cambridge University Press, 2014.
- [16] D. Lynden-Bell. Statistical mechanics of violent relaxation in stellar systems. *MNRAS*, 136:101, 1967.
- [17] R. M. Pengelly and M. J. Seaton. Recombination spectra, II. *MNRAS*, 127:165, 1964.
- [18] L. Spitzer. *Dynamical evolution of globular clusters*. Princeton, NJ, Princeton University Press, 1987.
- [19] D. B. Melrose. *Instabilities in Space and Laboratory Plasmas*. Cambridge, UK: Cambridge University Press, March 1989.

Thermodynamically-consistent semi-classical ℓ -changing rates

R. J. R. Williams¹, F. Guzmán², N. R. Badnell³,
P. A. M. van Hoof⁴, M. Chatzikos², G. J. Ferland³

¹ AWE plc, Aldermaston, Reading RG7 4PR, UK

² Department of Physics and Astronomy, University of Kentucky, Lexington, KY 40506, USA

³ Department of Physics, University of Strathclyde, Glasgow G4 0NG, UK

⁴ Royal Observatory of Belgium, Ringlaan 3, 1180 Brussels, Belgium

Abstract. We compare the results of the semi-classical (SC) and quantum-mechanical (QM) formalisms for angular-momentum changing transitions in Rydberg atom collisions given in a series of papers by Vrinceanu et al, most recently Vrinceanu, Onofrio & Sadeghpour, *ApJ* **747**, 56 (2012), with those of the SC formalism using a modified Monte Carlo realization. We find that this revised SC formalism agrees well with the QM results. This provides further evidence that the rates derived from the QM treatment are appropriate to be used when modelling recombination through Rydberg cascades, an important process in understanding the state of material in the early universe. The rates for $\Delta\ell = \pm 1$ derived from the QM formalism diverge when integrated to sufficiently large impact parameter, b . Further to the empirical limits to the b integration suggested by Pengelly & Seaton, *MNRAS* **127**, 165 (1964), we suggest that the fundamental issue causing this divergence in the theory is that it does not fully cater for the finite time taken for such distant collisions to complete.

PACS numbers: 32.80.Ee, 34.10.+x, 34.50.Fa

Submitted to: *J. Phys. B: At. Mol. Opt. Phys.*

1. Introduction

There has been significant recent interest in the rates for angular momentum changing collisions of low velocity ions with Rydberg atoms. While this may seem a somewhat obscure corner of atomic physics, the time to pass through the ladder of high-angular momentum levels in highly excited atoms proves to be a bottleneck in the process of atomic (re-)combination in the early universe. The details of the ℓ -changing rates therefore have a major impact on our understanding of this important stage in cosmic development [1].

For this Stark mixing process to be the dominant, the impact parameter of the collision must be sufficiently large that both the orbital quantum number within the target does not change, and the field due to the collider ion must remain smaller than that of the host nucleus throughout the interaction [2].

The atomic physics of these rates can be calculated by a variety of approximations, developing from classical orbit [3, 4, 5] to quantum orbit theory [6, 7, 8, 2, 9, 10]. In what follows we will refer to [2] and [10] as VF01 and VOS12, respectively. In this paper, we will concentrate on the differences between the most detailed of these formulations, those based on treating the response of the target orbital using quantum-mechanical perturbation theory (QM) and classical trajectory theory (SC). As discussed elsewhere ([11, 12], and references therein), these theories result in predictions for integrated rates which differ by up to an order of magnitude, sufficient to have a major impact on the interpretation of observations. This difference is primarily the result of the different range in impact parameter over which $|\Delta\ell| = 1$ transitions are active in the different theories: the QM theory has a logarithmic divergence in transition rate, which requires a limit to be placed on the largest impact parameter for which collisions are active in causing transitions, while in the SC approach as applied by VF01/VOS12, this limit arises as a result of the finite domain in impact parameter over which a single collision can cause a complete $|\Delta\ell| = 1$ transition.

In this paper, we will present the results of calculations using the semi-classical theory of VF01, but using Monte Carlo trajectory binning [13, 6]. We find that with this alternative approach, the SC results agree well with those of the quantum theory. So far as there are differences, these are as would be expected when relating a quantum theory to its classical limit, and are consistent with the correspondence principle. When integrated over impact parameter, b , and a thermal spectrum of colliders, it is clear that the differences in rates computed using this modified SC approach and the original QM formalism will be minimal.

In Section 2 we present the background theory, and in Section 3 compare the QM transition probabilities with SC probabilities as calculated by VF01 and VOS12, and with our revised approach. In Section 4, we briefly discuss how the discretely-sampled VF01 SC approach can be made somewhat more accurate, and consistent with the discrete detailed balance relations. Finally, in Section 5, we summarize our results, and discuss the processes which prevent the overall dipole transition rate from diverging in

a plasma of finite density.

2. Theory

VF01 and VOS12 provide detailed formulae for the rates of transitions $\ell \rightarrow \ell'$ for precise values of ℓ, ℓ' . They derive their semi-classical formulae using approximations which correspond to the continuum limit $n, \ell, \ell' \rightarrow \infty$, with ℓ/n and ℓ'/n finite, and then apply them in the case of finite quantum numbers. They apply what they term as a microcanonical ensemble, sampling the fundamentally continuous classical-limit expressions at discrete values of incoming and outgoing angular momentum appropriate for the angular momentum quantum number. Using this procedure provides values for the overall collision rate which are finite for all $\Delta\ell$, as noted above.

The process of returning from the continuum to the discrete limit is not, however, unique. In the present paper, we use a method similar to that discussed by [13]. To ensure thermodynamic consistency for the derived total rates, it is better to follow a finite-volume formalism (see, e.g., [14]), where each of the discrete quantum numbers is taken to correspond to a finite range of continuum values. The simplest assumption which will ensure results are consistent with the thermodynamical equilibrium is to assume that the probability density of states in the continuum band corresponding to each of the aggregate states is internally in thermodynamic equilibrium. As there is no energy difference between states in the case considered by Vranceanu et al., this corresponds to assuming a uniform population. This procedure provides results consistent with the thermodynamic requirements of unitarity and detailed balance and with the quantum and classical limits, as well as with usual practice in Monte Carlo simulation of off-lattice systems [15]. However, it leaves us looking to statistical physics, rather than numerical convention, to understand how to prevent the dipole transition rates from diverging as a result of the long-range nature of the Coulomb interaction.

For the standard quantum mechanical association of the radial quantum number n , the total angular momentum quantum number ℓ satisfies $0 \leq \ell \leq n - 1$. If we assume that each value of ℓ maps to a shell with total angular momentum between $\ell\hbar$ and $(\ell + 1)\hbar$, with a classical density of states $\propto \ell$ (which may be visualized as a two-dimensional polar coordinate system), then the area of this shell is $\propto 2\ell + 1$. This is consistent with the number of z -angular momentum eigenstates $|m| \leq \ell$ corresponding to each total angular momentum eigenstate. It results in a mean-squared angular momentum in the shell of

$$\langle L^2 \rangle = \left[\ell(\ell + 1) + \frac{1}{2} \right] \hbar^2, \quad (1)$$

which is a constant $\hbar^2/2$ greater than the value which enters in quantum mechanical calculations, $\langle L^2 \rangle = \ell(\ell + 1)\hbar^2$. For comparison, assuming that the total angular momentum corresponding to a quantum number ℓ is exactly $\ell\hbar$ underestimates $\langle L^2 \rangle$ by $\ell\hbar^2$, which is a significantly larger error for large ℓ . [Taking the angular momentum for the discrete state to be $(\ell + \frac{1}{2})\hbar$ is more accurate, with the classical and quantum

Thermodynamically-consistent semi-classical ℓ -changing rates

4

density of states being equivalent, and the mean-square angular momentum $\langle L^2 \rangle$ overestimated by $\hbar^2/4$.]

Transition probabilities in the finite volume regime can be derived from the semi-classical results of VF01/VOS12 by interpreting them as probability density functions in the continuum limit, so the transition probability from the state (n, ℓ) to (n, ℓ') becomes

$$\langle P^{\text{SC}} \rangle_{n\ell\ell'} = \frac{\int_{\ell/n}^{(\ell+1)/n} d\lambda \int_{\ell'/n}^{(\ell'+1)/n} d\lambda' P^{\text{SC}}(\lambda, \lambda', \chi) g(\lambda) g(\lambda')}{\int_{\ell/n}^{(\ell+1)/n} d\lambda g(\lambda)}, \quad (2)$$

where $g(\lambda) = 2\lambda$ is the classical density of states, normalized so that $\int_0^1 g(\lambda) d\lambda = 1$, and

$$P^{\text{SC}}(\lambda, \lambda', \chi) = \frac{2\lambda'/n}{\pi\hbar \sin \chi} \begin{cases} 0, & |\sin \chi| < |\sin(\eta_1 - \eta_2)| \\ \frac{K(B/A)}{\sqrt{A}}, & |\sin \chi| > |\sin(\eta_1 + \eta_2)| \\ \frac{K(A/B)}{\sqrt{B}}, & \text{otherwise,} \end{cases} \quad (3)$$

is the SC transition probability given by VOS12. In this expression, K is the complete elliptic integral,

$$A = \sin^2 \chi - \sin^2(\eta_1 - \eta_2), \quad (4)$$

$$B = \sin^2(\eta_1 + \eta_2) - \sin^2(\eta_1 - \eta_2), \quad (5)$$

$$\cos \eta_1 = \lambda, \quad (6)$$

$$\cos \eta_2 = \lambda', \quad (7)$$

and χ is given in terms of n and other implicit parameters of the collision by

$$\cos \chi = \frac{1 + \alpha^2 \cos(\sqrt{1 + \alpha^2} \Delta\Phi)}{1 + \alpha^2}, \quad (8)$$

$$\alpha = \frac{3Z_1}{2} \left(\frac{a_n v_n}{bv} \right), \quad (9)$$

where the swept angle $\Delta\Phi$ is assumed to be $-\pi$, and the Stark mixing parameter α depends on the average radius and velocity, a_n and v_n of the target orbital, as well as the charge $Z_1 e$, impact parameter b and velocity v of the impinging ion.

This procedure replaces the closed-form expressions of VF01 and VOS12 with a double integral, so is not as suitable for numerical work. However, it seems worthwhile to compare the results with those of the discrete interpretation in order to inform possible modifications to the VF01/VOS12 formalism which might be made to ensure compatibility with the limit of thermodynamic equilibrium.

1
2
3 *Thermodynamically-consistent semi-classical ℓ -changing rates*

5

4
5 There are a number of desirable properties for any set of approximate transition
6 probabilities. These include unitarity, i.e. that the system must reside in one of the
7 angular momentum states at the end of the transition
8

$$\sum_{\nu} P_{n\ell\nu} = 1, \quad (10)$$

9
10 and detailed balance, i.e.

$$(2\ell + 1)P_{n\ell\ell'} = (2\ell' + 1)P_{n\ell'\ell}, \quad (11)$$

11
12 for the quantum level degeneracy $g(\ell) = 2\ell + 1$. Note that the sum for the unitarity
13 requirement includes the probability that the scattering leads to no transition, $P_{n\ell\ell'}$ with
14 $\ell' = \ell$. It is possible to determine this rate using the same analytic forms as for the
15 ℓ -changing interactions, and this rate is included in the plots shown below.
16
17

18 The symmetry of the expressions for A and B in λ and λ' , together with the
19 overall factor of λ' in equation (3), means that equation (3) satisfies the detailed balance
20 relations *in the continuum limit*,

$$2\lambda P^{\text{SC}}(n, \lambda, \lambda') = 2\lambda' P^{\text{SC}}(n, \lambda', \lambda), \quad (12)$$

21 given the classical density of states $g(\lambda) = 2\lambda$. As a result of this, it is simple to verify
22 that the phase-space average, equation (2), satisfies the discrete detailed balance relation
23

$$(2\ell + 1) \langle P^{\text{SC}} \rangle_{n\ell\ell'} = (2\ell' + 1) \langle P^{\text{SC}} \rangle_{n\ell'\ell}. \quad (13)$$

24
25 Beyond these absolute requirements, we also suggest that the rates should be
26 subject to another statistical requirement for collisions at small impact parameter.
27 For these scatterings, the output state of the interaction is dependent on complex
28 interference phenomena, sensitive to many details of the atomic physics. However, the
29 net effect of this complexity, when averaged over some small range of incoming particle
30 properties, would be expected to be asymptotically close to the output states being in
31 statistical equilibrium (cf., for the classical case, [16]). We therefore suggest that, in the
32 limit of close scatterings $b \rightarrow 0$, the rates should be subject to an ergodicity property
33

$$\langle P \rangle_{n\ell\ell'} \simeq \frac{2\ell' + 1}{n^2}, \quad (14)$$

34 i.e. when the collider passes close enough to the core of the target atom, in the Stark
35 Adiabatic region, the effect of the collision is to randomize the output state, when the
36 input state is coarse-grained over a suitable domain. Of course, in reality scatterings
37 will cease to be purely ℓ -changing in this limit. Even so, it is to be expected that the
38 output state angular momentum will become statistically independent within the shell.
39 This requirement seems to be the best physical interpretation which can be put on the
40 statement in [17], hereafter PS64, that in the core the scattering probability becomes a
41 rapidly-oscillating function with mean value $\frac{1}{2}$. This is what would result from the core
42 ergodicity principle in the case of a two-level system, so the core ergodicity principle
43 seems like a reasonable generalization, agreeing with the work of PS64 at least in spirit.
44 As we will see, it is also a reasonable description of what in fact happens when the
45 quantum and shell-averaged classical transition probabilities are calculated in detail.
46
47
48
49
50
51
52
53
54
55
56
57
58
59
60

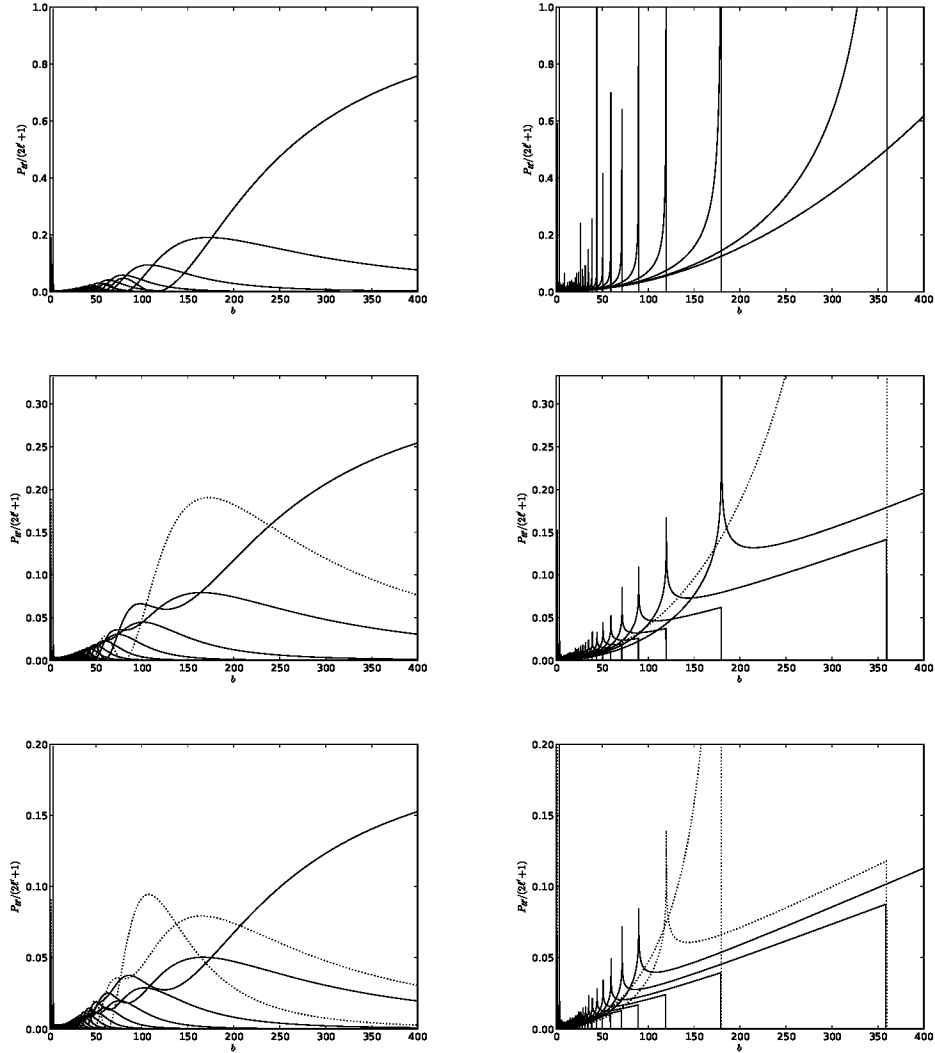


Figure 1. Plots of $P_{nl\ell'}/(2\ell'+1)$ vs b for $n = 30$ and $\ell = 0$ (first row), $\ell = 1$ (second row) and $\ell = 2$ (third row). The Stark parameter is $\alpha = 6/b$. Left column is using the QM formalism, right is using the SC formalism. The highest curve at large b has $\Delta\ell = 0$, larger $\Delta\ell$ curves appear in order as b reduces. Dotted curves are for $\ell' < \ell$.

3. Results

3.1. Comparison of QM and SC theory for fixed quantum numbers

In Figures 1 and 2, we compare the quantum mechanical probability distributions with the SC transition probabilities sampled at specific ℓ, ℓ' . The QM dipole transition rates, $\Delta\ell = \pm 1$ decay slowly as b increases, which is the origin of the divergence of the rate integral for these transitions. The SC transition probabilities show sharp edges where the transitions first become allowed, for all $\Delta\ell$: the transition rates for all $\Delta\ell$ are similar, as there is nothing in the SC formulation which fundamentally distinguished a $|\Delta\ell| = 1$ transition from one with a larger change in angular momentum. There are also internal

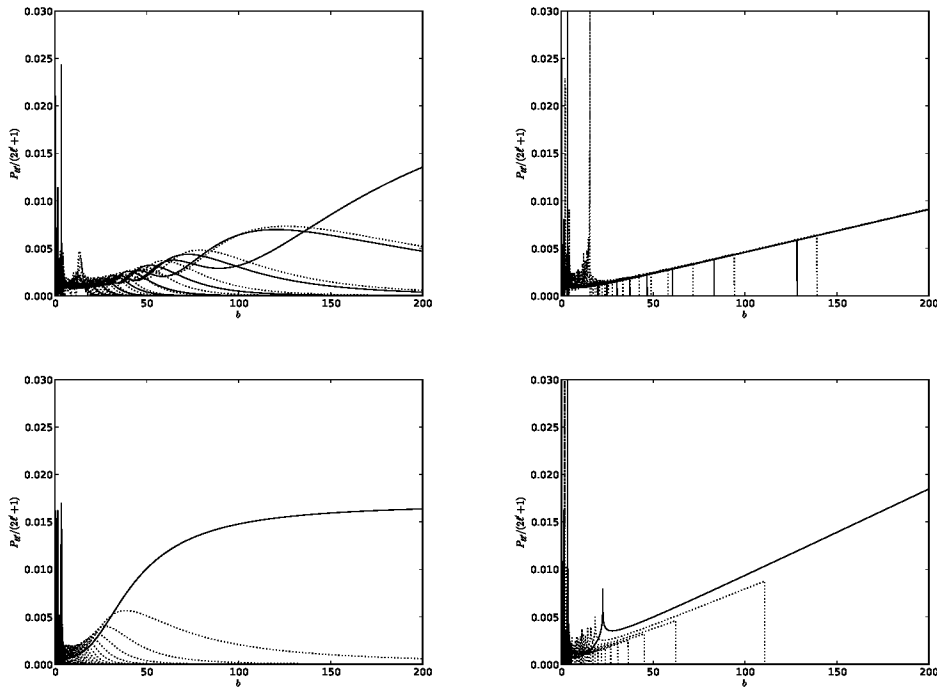


Figure 2. Plots of $P_{n\ell\ell'}/(2\ell'+1)$ vs b for $\ell = 20$ (first row) and $\ell = 29$ (second row). The n and α parameters are as in Figure 1. Left column is using the QM formalism, right is using the SC formalism. Dotted curves are for $\ell' < \ell$. Note that there are no upward transitions for $\ell = 29$ due to the constraint that $\ell' < n$.

peaks for many cases, corresponding to orbital resonances. These are used by VOS12 to limit the domain over which $|\Delta\ell| = 1$ transitions are allowed, avoiding the divergence in the integrated transition rate found for the QM dipole transition rate.

It is clear that the SC transition probabilities cannot satisfy unitarity, as where any transition ceases to be allowed, there is no corresponding increase in the others. Indeed, at sufficiently large radii, the probability of no transition, $P_{n\ell\ell}$, increases above unity, which is inconsistent with usual definition of probability. The quantum transition probabilities do satisfy unitarity (note that the curves as plotted are divided by $2\ell'+1$ to make the ergodicity property at small b more obvious, but this means that this summation property for the probabilities is less obvious as shown).

In Figures 3 and 4, we compare the quantum mechanical probability distributions with the SC probability distributions averaged over angular momentum shells. These plots are significantly more alike than those for the comparison between the quantum mechanical probability and the discretely-sampled SC transition probability. While there are no longer any sharp edges in the shell-averaged SC probabilities, for $|\Delta\ell| > 1$ they will be non-zero only within some range of α values. (The integration over a quantized shell width means that there is now a genuine distinction in qualitative behaviour between transitions with different $|\Delta\ell|$.) The shell-averaged SC probabilities also satisfy unitarity and the quantum-weighted detailed balance constraint.

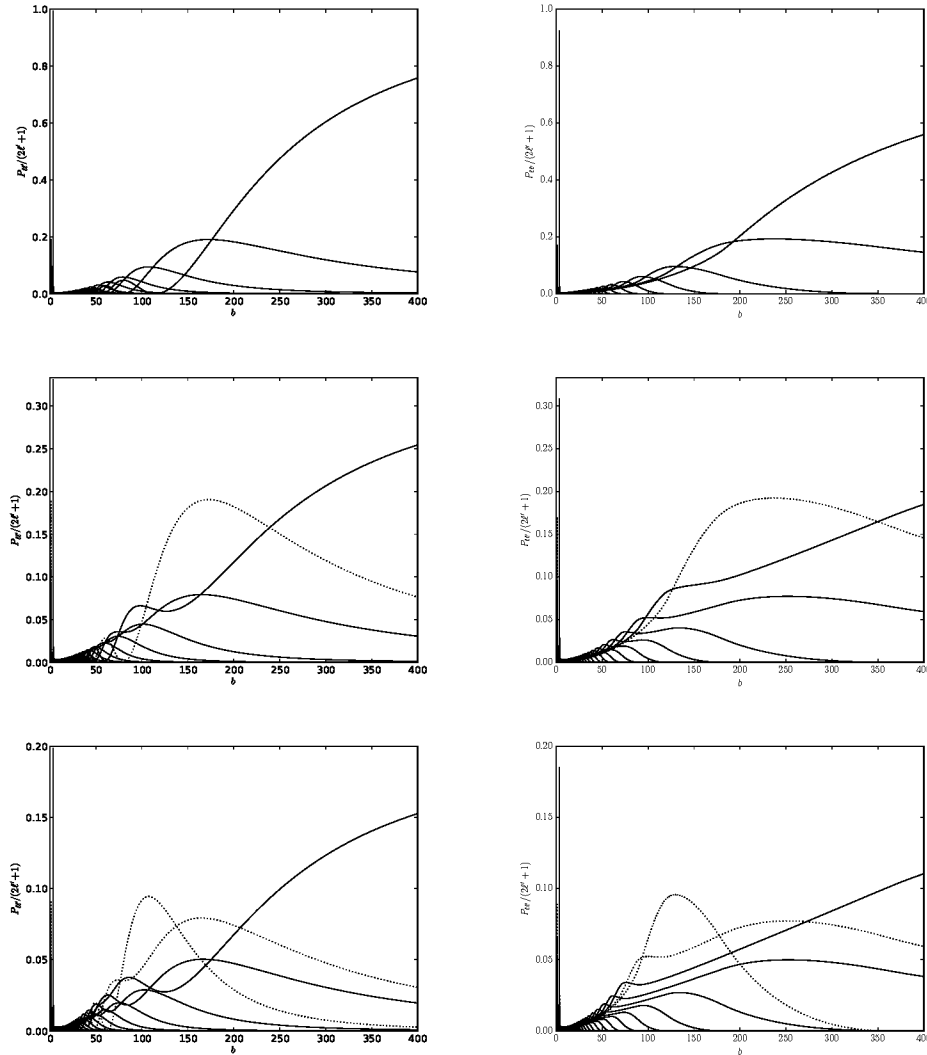


Figure 3. Plots of $P_{n\ell\ell'}/(2\ell'+1)$ vs b for $\ell = 0$ (first row), $\ell = 1$ (second row) and $\ell = 2$ (third row). Left column is using the QM formalism, right is using the SC formalism, averaged over shells. Dotted curves are for $\ell' < \ell$.

Away from the region where the discretely-sampled transition probability is zero, the binning has a relatively minor effect, simply smoothing out the steepest peaks.

The general form of the transition probability distributions shown in these figures is of interest. Working from large b inwards, it is initially most likely that no change in ℓ will result. At least in the QM case, all other values of $\Delta\ell$ are possible, with probabilities reducing as $|\Delta\ell|$ increases. As b becomes smaller, the probabilities of the higher $|\Delta\ell|$ transitions increase, following a smooth power law dependency, until the statistical weight of the output state reaches a similar level to that of the $\Delta\ell = 0$ transition. Thereafter, the probabilities are subject to significant oscillations, around an average level consistent with statistical balance, apart from a strong spike at the very smallest values of b . This suggests that the combination of the asymptotic behaviour at large b , the core ergodicity

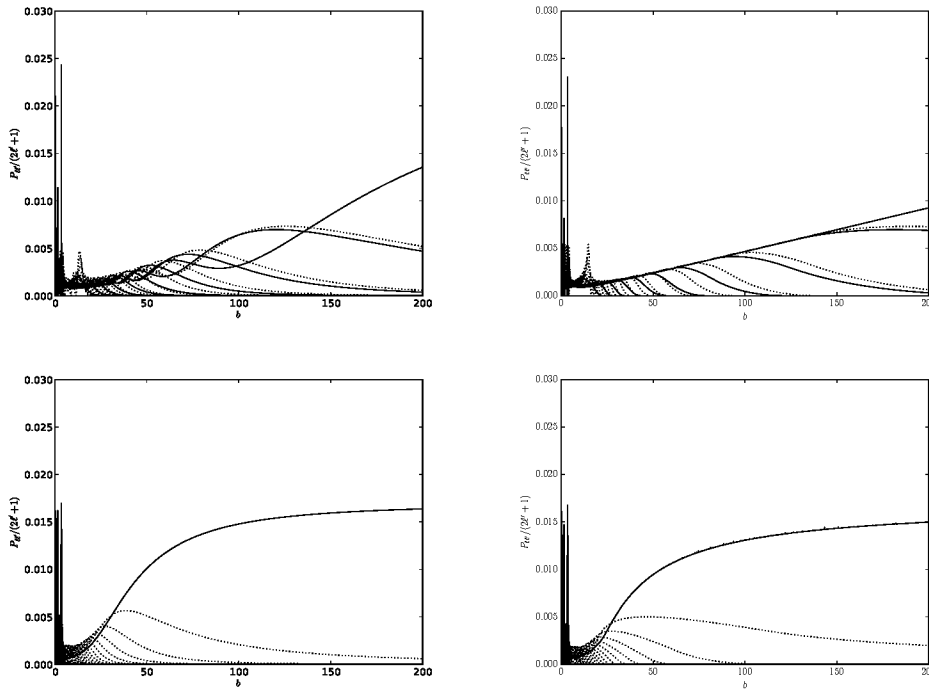


Figure 4. Plots of $P_{n\ell\ell'}/(2\ell'+1)$ vs b for $\ell = 20$ (first row) and $\ell = 29$ (second row). Left column is using the QM formalism, right is using the SC formalism, averaged over shells. Dotted curves are for $\ell' < \ell$.

principle, and the fundamental requirements of unitarity and detailed balance, should be sufficient to provide thermodynamically-consistent estimates of the impact-parameter and thermal-averaged rates which would be acceptably accurate for many applications.

3.2. The classical limit of the QM formalism

Having shown that the SC results can be made acceptably consistent with those of the QM formalism by an appropriate binning procedure, it is also of interest to demonstrate consistency in the opposite direction. To do this, in Figure 5, we compare the non-averaged SC probability for one transition with a series of QM results with quantum numbers increasing by factors of 2. As the quantum numbers increase, while maintaining their ratios, the QM results tend to the SC limit, with the resolution of sharp features, including the orbital resonances seen in the classical results, gradually improving. Oscillations remain within the classically-allowed range, and long tails in the classically-forbidden range. This combination of Gibbs phenomenon ringing and evanescent tunnelling behaviour, typical of the Airy function, is characteristic of the classical limit of quantum phenomena. The QM formalism remains accurate for all values of the quantum numbers, but the expressions for the rates become increasingly difficult to evaluate numerically.

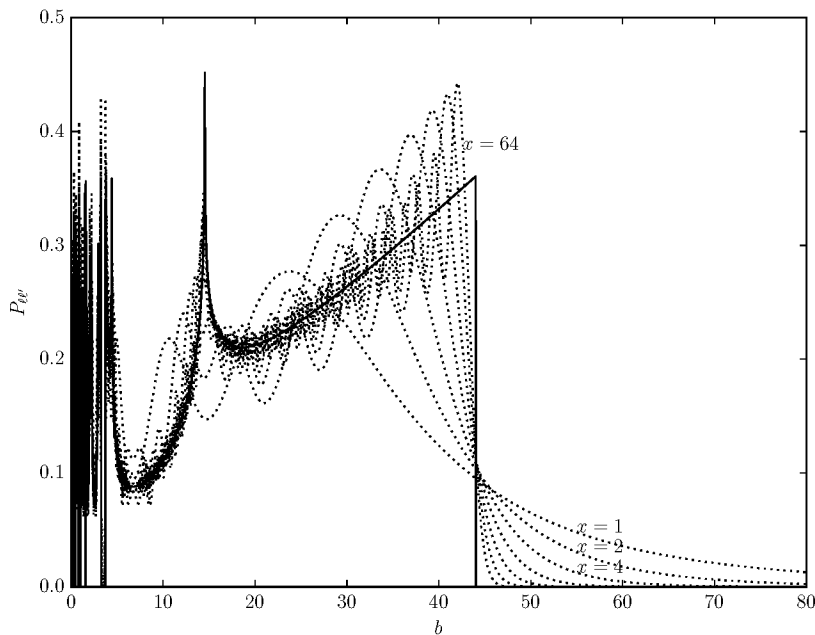


Figure 5. Comparison of the SC $P_{n\ell\ell'}$ vs b for $\ell = 2$, $\ell' = 4$, $n = 8$ transition probability (solid line), compared to a succession of scaled QM formalism probabilities $xP_{n\ell\ell'}$, with $\ell = 2x$, $\ell' = 4x$ and $n = 8x$, where $x = 1, 2, 4, 8, \dots, 64$. As the scaling factor x increases, the QM probabilities tend towards the SC results.

4. Use of semi-classical probabilities

The shell-sampled probabilities presented in the previous section are determined using a computationally expensive double integral. It may be possible to perform one or both of these integrals analytically, but numerical results were sufficient for the present analysis.

However, given that the use of a classical transition rate is already a significant approximation, using a point sample of the transition rate rather than an integral is likely to be an acceptable approximation, at least away from the case of $\Delta\ell = \pm 1$, $b \rightarrow \infty$. As these rates are being attributed to quantum mechanical rather than classical states, it makes sense to ensure the rates are chosen so as to satisfy quantum mechanical rather than classical statistics. The most consistent identification of quantum mechanical states with a continuum band has $\ell\hbar$ as the angular momentum at the innermost edge of the band. Hence, if a single value based on the classical transition probability is to be used for this quantum number, it will be accurate to a higher order if the angular momentum used in this expression is somewhat higher than $\ell\hbar$. In particular, in order to be consistent with the quantum mechanical detailed balance condition, the value $2\ell' + 1$ should be used in the numerator of the prefactor of equation (6) of VOS12. This means that the $\ell \rightarrow \ell' = 0$ rates will not be strictly zero, as required by the expressions given by VF01. Given that VF01 provide expressions for the transition rate *out* of an

$\ell = 0$ state, a zero inward rate is in clear violation of the detailed balance requirement.

The values used in the elliptic integral terms must be symmetric functions of ℓ, ℓ' , as is true for the expressions given. Ideally they should also be chosen to satisfy unitarity, but in reality the correction to the overall transition rates as a result of violating this constraint will be small compared to the other approximations underlying this approach. Using $\cos \eta_1 = (\ell + \frac{1}{2})/n$, etc., will be at least somewhat more accurate than without the $\frac{1}{2}$, and also means that the cases $\ell = 0, \ell' = 0$ do not require a special treatment.

5. Conclusions

We have shown that, by using an alternative form for the Monte Carlo realization, the results for the SC and QM formalisms described by VF01 and VOS12 can be brought closely into line. As this is consistent with what is expected as a result of the correspondence principle, it provides further evidence that the results of the QM formalism of VF01 and VOS12 is accurate, and should be preferred over their SC formalism in regimes where their results differ significantly.

While finding agreement between the different forms of theory is satisfying, this does not take into account the major reason given by VF01 and VOS12 for preferring their semi-classical results, specifically the need for an outer limit to be imposed on the integration over impact parameters to prevent the total collision rate diverging for $\Delta\ell = \pm 1$ when using the QM theory. This type of divergence is common in other areas of collision rate physics (in particular, the two-body relaxation time, [18, 19]), so is not unexpected. PS64 give expressions for a variety of empirical limits to the range of b over which Stark mixing will be active, due to Debye screening, target atom state radiative lifetimes, and the lifting of degeneracy between the ℓ levels as a result of relativistic effects, or the finite core radius for target atoms of species heavier than H. The value of the outer cut-off is taken to be the most constraining of these processes. The logic here is similar to the outer limit applied to the Coulomb logarithm in other contexts, such as two-body relaxation in plasmas. The relevant Debye screening is that which reduces the long-range field of the impinging ion (Debye screening of the charge of the target atom nucleus is in effect a continuum lowering process), and will be rapid for colliders with thermal velocities due to the high mobility of electrons.

Nevertheless, it is also worth noting that as b increases, so does the time over which the collision takes place: the treatment of collisions as independent events must therefore eventually become inaccurate. During the extended period taken to complete the most distant encounters, there will be time for many collisions at smaller impact parameters. While, at first order, the effects of collisions will superpose linearly, at sufficiently large b a limit will be reached where smaller impact parameter collisions together are sufficient to randomize the angular momentum of the target orbital during the time over which the larger b interaction is taking place. Once b increases above the level where this occurs, b_{eq} , the effect of collisions at larger impact parameter will be felt, in effect, as a superposition of $N_{\text{coll}} \sim \tau_{\text{coll}}/\tau_{\text{eq}}$ partial interactions adding in quadrature, rather

than linearly (where τ_{coll} is the collision time at the large b of interest, and τ_{eq} is the collision time at the smallest radius leading to effective randomization). A reduction in contribution to the transition probability by $\sim N_{\text{coll}}^{-1/2} \propto b^{-1/2}$ at the largest b will be sufficient to prevent the weak logarithmic divergence in the overall rate. This is a somewhat academic argument, as the plasma particle correlations underlying Debye screening will in general result in more stringent limits to the range of b over which collisions are effective. Nevertheless, given that the agreement we now find between the SC and QM gives greater confidence in SC results for the Rydberg scattering problem, it may be possible to investigate the corrections required for these multiple interactions in a believable manner using explicit classical trajectory calculations.

Acknowledgements

We thank D. Vranceanu and H. Sadeghpour for helpful responses to several queries about their published work, and the referees for valuable suggestions. Parts of this work have been supported by the NSF (1108928, 1109061, and 1412155), NASA (10-ATP10-0053, 10-ADAP10-0073, NNX12AH73G, and ATP13-0153), and STScI (HST-AR-13245, GO-12560, HST-GO-12309, GO-13310.002-A, and HST-AR-13914). MC has been supported by STScI (HST-AR-14286.001-A). PvH was funded by the Belgian Science Policy Office under contract no. BR/154/PI/MOLPLAN.

- [1] J. Chluba and R. A. Sunyaev. Induced two-photon decay of the 2s level and the rate of cosmological hydrogen recombination. *A&A*, 446:39–42, January 2006.
- [2] D. Vranceanu and M. R. Flannery. Classical and quantal collisional Stark mixing at ultralow energies. *Phys. Rev. A*, 63(3):032701, March 2001.
- [3] I. C. Percival and D. Richards. Classical theory of transitions between degenerate states of excited hydrogen atoms in plasma. *Journal of Physics B Atomic Molecular Physics*, 12:2051–2065, June 1979.
- [4] A. K. Kazansky and V. N. Ostrovsky. Classical theory of ℓ -changing transitions in collisions between Rydberg atoms and ions. *Phys. Rev. A*, 52:R1811–R1814, September 1995.
- [5] A. K. Kazansky and V. N. Ostrovsky. Rydberg-atom - ion collision: classical theory of intrashell transitions. *Journal of Physics B Atomic Molecular Physics*, 29:3651–3672, August 1996.
- [6] AK Kazansky and VN Ostrovsky. Rydberg atom-ion collisions: Quantum theory of intrashell transitions. *Physical review letters*, 77(15):3094, 1996.
- [7] D. Vranceanu and M. R. Flannery. Classical Stark Mixing at Ultralow Collision Energies. *Physical Review Letters*, 85:4880–4883, December 2000.
- [8] D. Vranceanu and M. R. Flannery. LETTER TO THE EDITOR: Quantal Stark mixing at ultralow collision energies. *Journal of Physics B Atomic Molecular Physics*, 33:L721–L728, October 2000.
- [9] D. Vranceanu and M. R. Flannery. LETTER TO THE EDITOR: Analytical quantal collisional Stark mixing probabilities. *Journal of Physics B Atomic Molecular Physics*, 34:L1–L8, January 2001.
- [10] D. Vranceanu, R. Onofrio, and H. R. Sadeghpour. Angular Momentum Changing Transitions in Proton-Rydberg Hydrogen Atom Collisions. *ApJ*, 747:56, March 2012.
- [11] F. Guzmán, N. R. Badnell, R. J. R. Williams, P. A. M. van Hoof, M. Chatzikos, and G. J. Ferland. H, He-like recombination spectra - I. ℓ -changing collisions for hydrogen. *MNRAS*, 459:3498–3504, July 2016.
- [12] F. Guzmán, N. R. Badnell, R. J. R. Williams, P. A. M. van Hoof, M. Chatzikos, and G. J.

- 1
2
3
4
5 Ferland. H-, He-like recombination spectra - II.l-changing collisions for He Rydberg states.
6 MNRAS, 464:312–320, January 2017.
- 7 [13] R. L. Becker and A. D. MacKellar. Theoretical initial l dependence of ion-Rydberg-atom collision
8 cross sections. *Journal of Physics B Atomic Molecular Physics*, 17:3923–3942, October 1984.
- 9 [14] Randall J LeVeque. *Finite volume methods for hyperbolic problems*, volume 31. Cambridge
10 University Press, 2002.
- 11 [15] David P Landau and Kurt Binder. *A guide to Monte Carlo simulations in statistical physics*.
12 Cambridge University Press, 2014.
- 13 [16] D. Lynden-Bell. Statistical mechanics of violent relaxation in stellar systems. MNRAS, 136:101,
14 1967.
- 15 [17] R. M. Pengelly and M. J. Seaton. Recombination spectra, II. MNRAS, 127:165, 1964.
- 16 [18] L. Spitzer. *Dynamical evolution of globular clusters*. Princeton, NJ, Princeton University Press,
17 1987.
- 18 [19] D. B. Melrose. *Instabilities in Space and Laboratory Plasmas*. Cambridge, UK: Cambridge
19 University Press, March 1989.
- 20
21
22
23
24
25
26
27
28
29
30
31
32
33
34
35
36
37
38
39
40
41
42
43
44
45
46
47
48
49
50
51
52
53
54
55
56
57
58
59
60